

Fast ion Collective Thomson Scattering diagnostic for TEXTOR

H Bindslev^a, L Porte^b, A Hoekzema^c,
J Machuzak^b, P Woskov^b, D Van Eester^d

^a FOM Instituut voor Plasmafysica, Rijnhuizen, EURATOM Association, Postbus 1207, NL-3430 BE Nieuwegein, The Netherlands*. ^b MIT Plasma Science and Fusion Center, Cambridge, MA 02139, USA. ^c Institut für für Plasmaphysics, Forschungszentrum Jülich GmbH, EURATOM Association, D-52425 Jülich, Germany*. ^d Laboratory for Plasma Physics, Euratom Association, Koninklijke Militaire School/Ecole Royale Militaire, Belgium*.
*partner in the Trilateral Euregio Cluster

Introduction. A Collective Thomson Scattering diagnostic is being built for diagnosing confined fast ions in the TEXTOR tokamak. With this we intend to address both generic issues of energetic ion dynamics and specific issues for Ion Cyclotron Resonance Heating (ICRH). ICRH combined with Neutral Beam Injection is capable of producing highly non-thermal fast ion distributions in TEXTOR, where, for standard currents, deuterons with energies up to 400 keV can be confined. The probing radiation will be provided by a gyrotron delivering 350 kW for up to 200 ms at 110 GHz. Operating with a magnetic field of 2.6 Tesla the electron cyclotron emission (ECE) and other plasma noise in the relevant spectral range is negligible. This should permit 20 measurements per shot with a temporal resolution of 10 ms and adequate velocity space resolution. Initially a near back-scattering geometry will be implemented, providing a radial resolution of approximately 10 cm. Radial location of the measuring volume and direction of the resolved velocity component can be varied from shot to shot. Later an additional receiver will be installed providing near 90 degrees scattering angle. This facilitates simultaneous resolution of the 1-D velocity distributions near parallel and perpendicular to the magnetic field with a radial resolution in both cases of approximately 5 cm.

Mission. We intend to address both generic issues of energetic ion dynamics and specific issues of ICRH physics. The questions we hope to address include:

- Will the experimentally measured anisotropic ICRH fast ion velocity distributions agree with theoretical predictions, including the classic “rabbit ear” feature?
- What happens to the fast ions at the periodic and ever-present plasma profile relaxations (sawtooth crash)? Are they expelled from the core?
- Some of the recent improvements in bulk plasma confinement are achieved through modified magnetic configurations (reversed shear), for which theory predicts much increased fast ion ripple losses. This may negate the improved performance for the bulk and must be investigated.
- Will (fusion created) alpha particles absorb RF power when present in the reactor? Theory yields two conflicting answers: A) based on classical reasoning, predicts abundant alpha absorption. B) noting that alpha particles are not very collisional, concludes that there will be destructive interference of subsequent encounters of the particle with the cyclotron resonance layer, which results in no damping; this is the *superadiabatic regime*. We can address the question of alpha absorption by investigating whether there is a fast ion energy threshold above which heating becomes inefficient.

- Fast ion and ICRH models lack a good description of the drift effects responsible for radio wave induced transport. Cross-checking against experimental data will allow benchmarking of the theory and show where it needs to be refined.

Diagnostic design. The ECRH system, currently being constructed at TEXTOR, will provide the probing radiation. For the fast ion CTS the source will be a 110 GHz gyrotron capable of delivering 350 kW RF to the plasma for 200 ms. The probing beam, launched at the mid plane on the low field side, will be a focussed Gaussian with waist radius, $w_0 = 1.5$ cm. Beam focal length will be variable and the beam direction steerable, toroidally and poloidally. Elliptical polarisation will be selected by a universal polariser to match the plasma modes (O or X). Scattered radiation is received by two antennae. No. 1 placed at nearly the same toroidal location as the ECRH launcher and at a poloidal angle of 24.2° above the launching antenna. No. 2 is located at a toroidal angle of -42.7° relative to the launcher and a poloidal angle of 19.1° above the mid plane. The geometry is illustrated in Figure 1.

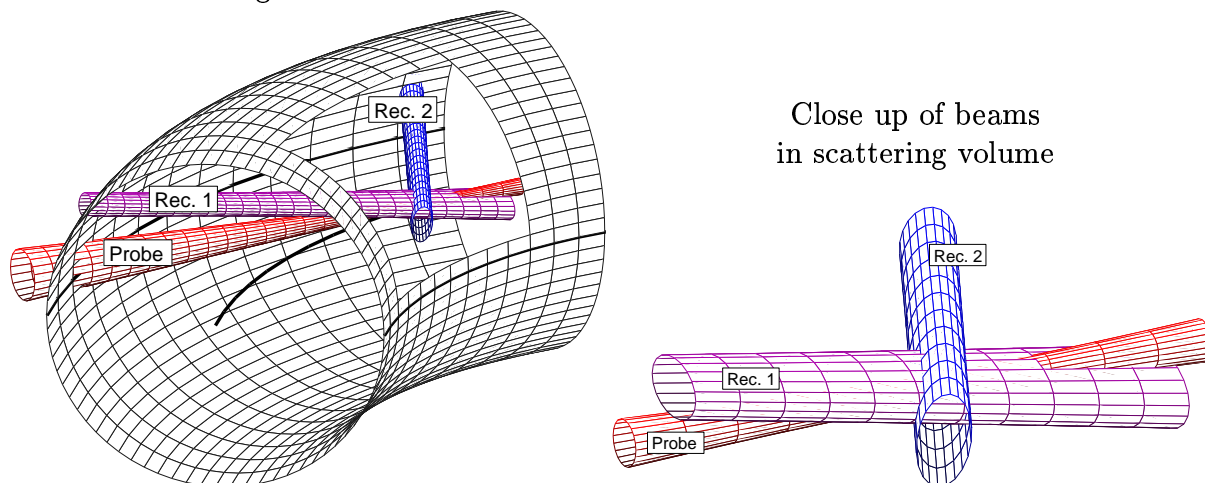


Figure 1: Geometry of the TEXTOR fast ion CTS diagnostic. The plasma centre and midplane at the plasma edge are indicated by fat black curves. Receiver beam patterns are widened in the direction out of the plane spanned by the probing beam and the respective receiver beam.

The directions of the receiver beams are steerable, toroidally and poloidally. The received polarisations will also be selected by universal polarisers. The beam patterns of the receiving antennae will be anisotropic Gaussians, each focussed in the *beam plane* spanned by the probing beam and the respective receiver beam (vertical for receiver # 1 and near horizontal for receiver # 2). In these planes the waist half widths (field $1/e$) are approximately 3 cm, which are the minimum achievable given the limitations on receiver antennae apertures. These widths affect the sizes of the scattering volumes; for the scattering geometry shown in Figure 1 they determine the dimensions in the toroidal direction. The signal strengths are not affected by these widths.

Orthogonal to the beam planes we intend to expand the receiver beams to give waist half widths of approximately 6 cm in the scattering volume, as illustrated in Figure 1. This design is chosen to make the overlap of probing and receiver beams less sensitive to uncertainties in the actual and the required antenna orientations. It will also make the overlap more robust against sawteeth and other causes of variable refraction. This robustness comes at a cost to the CTS signal strength and thus the diagnostic information,

but it will reduce the uncertainty in the beam overlap, which can be the main source of uncertainty in the absolute calibration.

The detection system is super heterodyne with 40 channels for each of the two antennae. A notch filter placed before the first mixer attenuates the stray radiation. The antenna noise temperature of the receivers is estimated at 13 eV.

For initial operation (till summer 2000) only antenna # 1 will be operational. For this phase a compact Cassegrain design will be used. This design makes use of fundamental rectangular waveguide with a rectangular horn as feed, which implies that only horizontal linear polarisation is received. To ensure good coupling to the O mode, operation will in this phase be limited to geometries where the beam plane is near the poloidal plane.

Diagnostic potential. The steerability of probe and receiver beams permits localised measurements at nearly all poloidal locations. For the geometry shown in Figure 1 the radial and vertical resolution is principally determined by the width of the probing beam which is approximately 3 cm. For receiver 2 the toroidal resolution is determined by the receiver beam width in the beam plane. It is approximately 6 cm. For receiver 1 the toroidal resolution will be approximately 40 cm. Using receiver 1 in a geometry where its beam plane is near perpendicular to the magnetic field, the radial resolution of receiver 1 will be approximately 10 cm, while the vertical and toroidal resolution is 3 cm.

The operation of two receivers permits simultaneous measurement of the distributions of two near orthogonal velocity components; with the geometry illustrated in Figure 1, receiver 1 would resolve the distribution of velocities near parallel to the magnetic field while receiver 2 would resolve velocities near perpendicular to the field. Operating with the beam plane of receiver 1 near perpendicular to the magnetic field, receiver 1 will also resolve the perpendicular velocity component.

It is the intention to use O mode for both probe and receivers to minimise refraction. At an electron density of $5 \times 10^{19} \text{m}^{-3}$ refraction is negligible for near perpendicular propagation; refraction shifts receiver beam 2 by 1.5 cm in the plasma centre for the geometry shown in Figure 1. For near tangential propagation, as is the case for receiver 1 and probe in Figure 1, refraction shifts the beams by approximately 15 cm. The differential rate of refractive radial shift is $\partial R/\partial n_e = 5 \text{ cm}/10^{19} \text{m}^{-3}$. The rate is nearly identical for probe and receiver 1, implying that the overlap is robust in the event of density variations. The refractive shift of the probe is nearly in the beam plane of receiver 2, implying that the overlap with receiver 2 is also reasonably robust against density variations. The dispersive refraction for receiver 1 for tangential propagation is $\partial R/\partial \nu^s = 3 \text{ cm}/10 \text{ GHz}$. Here ν^s is the frequency of the received scattered radiation. The full spectral width will generally be on the order of 10 GHz (see Figure 2) so the dispersive refraction must be taken into account. This is an additional reason for the widening of the beam pattern of receiver 1.

With a Salpeter parameter, $1/(k^\delta \lambda_D)$, above 6 for back scattering, and $n_e = 5 \times 10^{19} \text{m}^{-3}$ and $T_e = 2 \text{ keV}$, we can rely on the fast ion feature dominating the electron feature for a wide range of fast ion phase space densities and scattering geometries[1]. This is brought out in Figure 2, which shows the predicted sensitivities of receiver 2 for the geometry in Figure 1. The CTS spectra are computed using the expressions given in Refs [2] and [3].

At a toroidal magnetic field of 2.6 Tesla the fundamental and second harmonic cyclotron resonances at 110 GHz are respectively on the high field and low field sides of the plasma, and both outside the plasma. At this field there is thus a local minimum in the

spectral power density of the ECE in the frequency range 100 to 120 GHz. Measurements with the existing ECE diagnostic at TEXTOR indicate a spectral power density of less than 5 eV. The antenna noise temperatures of the receivers are estimated to be less than 15 eV.

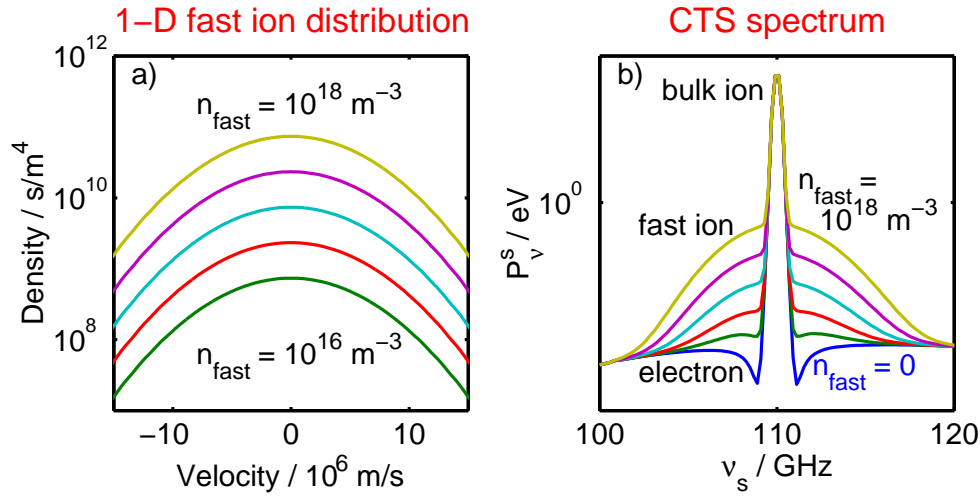


Figure 2: Sensitivity of the TEXTOR fast ion CTS diagnostic, receiver # 2 $\theta = 90^\circ$, $\phi = 60^\circ$. $P^i = 350$ kW, $n_e = 5 \times 10^{19} \text{ m}^{-3}$, $T_e = 2$ keV. The model fast H distributions used here are Maxwellian with a temperature of 300 keV.

Principal component analysis [4] reveals uncertainty in a scaling factor for the inferred fast ion distribution, which is due to uncertainties in beam overlap and a range of bulk plasma parameters. Uncertainty in the scaling factor is not particularly sensitive to the spectral signal to noise ratio and thus not significantly affected by changes in for instance integration time or noise temperature.

Without knowledge of the beam overlap or absolute calibration the uncertainty in the scaling factor reaches 50 %. The accuracies of the remaining components are around 1 for a target resolution of $\Delta = 10^9 \text{ s/m}^4$, a noise temperature of $T_N = 20$ eV, scattering angle of $\theta = 90^\circ$, and integration time of $\tau = 20$ ms. This implies that, apart from the uncertainty in the scaling factor, the remaining uncertainties, which are only weakly correlated, are below

$$\sigma_{\max} \approx 10^9 \text{ s/m}^4 \left(\frac{10^6 \text{ m/s}}{\Delta v} \right)^{1/2} \left(\frac{20 \text{ ms}}{\tau} \right)^{1/2} \frac{T_N}{20 \text{ eV}}$$

where Δv is the velocity space resolution. This can be compared with typical TEXTOR ICRH fast H distributions for which $E_{\max} = 0.5$ MeV, $v_{\max} = 10^7$ m/s, implying for instance that 20 nodes in the distribution could be resolved with an accuracy better than the target of 10^9 s/m^4 . The detection limit with 20 nodes and flat distribution is thus $2 \times 10^{16} \text{ m}^{-3}$

This work is partly funded by NWO, EURATOM and US-DOE.

References

- [1] E. E. Salpeter. *Physical Review*, **120**, 1528, (1960).
- [2] H. Bindslev. *Plasma Physics and Controlled Fusion*, **35**, 1615, (1993).
- [3] H. Bindslev. *J. Atmospheric and Terrestrial Physics*, **58**, 983, (1996).
- [4] H. Bindslev. In *Proc. of the 8th Int. Symp. Laser-Aided Plasma Diagnostics*, pages 265–276, Doorwerth, The Netherlands, 1997. (FOM “Rijnhuizen” 1997).